

A Study of Rheological Properties and Crystallization Behavior for HDPE Melts During Extrusion

J. N. NESS¹ and J. Z. LIANG^{2,*}

¹Department of Mechanical Engineering, University of Hong Kong, Hong Kong, and ²Department of Chemical Machinery, South China University of Technology, Guangzhou 510641, People's Republic of China

SYNOPSIS

The influence of temperature and shear rate on the flow behavior of high density polyethylene (HDPE) melts during extrusion has been investigated by using a Ceast Rheovis 2100 capillary rheometer which was manufactured by the Ceast Co. in Italy. It was found that the entry pressure drop for the samples was very low during extrusion, the relationship between shear stress and shear rate did not obey the power law strictly, and the phenomenon of shear-induced crystallization was easily produced when temperature was near the melting point of the samples, even though the shear rate was not high. The dependence of the shear viscosity for the samples on temperature can be described by using the Arrhenius equation.

© 1993 John Wiley & Sons, Inc.

INTRODUCTION

High density polyethylene (HDPE) is a typical crystallizability thermoplastic plastics. It is generally agreed that there is obvious difference in flow behavior and its mechanism for crystallizable and noncrystallizable polymer in processing. The high molecular structure of crystallizable polymer can change under given operating conditions. For instance, when the temperature is near the melting point of the materials the molecular chains are oriented along the direction of flow or drawing, and a crystallization phenomenon is produced during extending or spinning. It is called flow induced-crystallization. Several researchers¹⁻⁷ have studied the phenomenon of flow-induced crystallization and its mechanism for crystallizable polymer. Keller and his co-workers¹ started elucidating the subject early. They found that primary nucleation occurs a line, or row, rather than at a point while drawing HDPE melt. Lagasse and Maxwell² observed a relation between the induction time and shear rate as flow induced crystallization occurs. The results showed that

the induction time kept at an higher value (10–100 s) when shear rate was smaller than 1; and the induction time decreased quickly with increasing shear rate as shear rate was greater than 1. Southern and Porter³ have applied a combination of high pressure and flow orientation in structuring HDPE. The polymer was extruded at 134°C through a conical die that gave an effective draw ratio of 46. Since this temperature was below the prevailing melting point, because of orientation, the polymer crystallized in the die. To avoid to have crystallization occur in the entrance region to affect extrusion, Collier and his fellows⁴ applied steep temperature gradients, with temperature decreasing with increasing capillary length, and observed crystallization phenomenon as the chains were fairly well aligned. Akay⁵ investigated the subject about flow-induced orientation and diffusion for glass-fiber-reinforced polymer melt in capillary flow, and Morrison et al.⁶ researched flow-induced structure and rheology of a triblock copolymer (SBS). White⁷ reviewed the advance in polymer structure development in processing.

In this study, we investigated mainly the rheological properties of HDPE melts under near practical production operating conditions (shear rate and temperature), the critical extrusion conditions of onset of shear-induced crystallization, and the effect of the crystallization phenomenon on the processability and the flow behavior of the samples.

* To whom correspondence should be addressed at: Department of Chemical Machinery, South China University of Technology, Guangzhou 510641, People's Republic of China.

THEORETICAL CONSIDERATION

When a polymer melt is forced by the piston and enters a capillary die from a reservoir, the melt will produce the relevant extensional and shear flow. If the melt flow is steady and laminar and there is no slip at the die wall, then the shear stress (τ_w) at the wall can be expressed by the following equation:

$$\tau_w = \Delta P_c D / 4L \quad (1)$$

where D and L are the diameter and length of the capillary die, respectively, Q is the volumetric flow rate, and ΔP_c is the capillary die pressure drop. The apparent shear viscosity (η_a) of the melt is here defined as a ratio of shear stress to apparent shear rate ($\dot{\gamma}_a$):

$$\eta_a = \tau_w / \dot{\gamma}_a \quad (2)$$

and

$$\dot{\gamma}_a = 4Q / \pi R^3 \quad (3)$$

where Q is the volumetric flow rate and R the die radius.

Because of the non-Newtonian property for polymer melt, eq. (1) needs to be corrected as follows to obtain the true wall shear rate:

$$\dot{\gamma}_w = \frac{3n' + 1}{4n'} \dot{\gamma}_a \quad (4)$$

where

$$n' = d(\log \tau_w) / d(\log \dot{\gamma}_a) \quad (5)$$

Thus, the true shear stress at the wall can also be expressed as follows:

$$\tau_w = K' \dot{\gamma}_w^{n'} \quad (6)$$

According to the definition of viscosity via eq. (2), the viscosity of the melt is given by

$$\eta = K' \dot{\gamma}_w^{n'-1} \quad (7)$$

where K' is often known as the consistency index and n' is the flow behavior index, which is influenced by shear rate.

Hence, the true shear viscosity of the melt is given by

$$\eta = \frac{4n'}{3n' + 1} \eta_a \quad (8)$$

If the shear flow for the melt is strictly in keeping with the power law, then $n = n'$ and $K = K'$. Where K and n are the power law constants. The relationship between K' and K can be determined by the following expression,

$$K' = K \left(\frac{3n + 1}{4n} \right)^n \quad (9)$$

and a relationship between n and n' is given by⁸

$$n = n' / 1 - [1 / (3n' + 1)] (dn' / d \ln \tau_w) \quad (10)$$

where n' now refers to the shear stress τ_w .

EXPERIMENTAL

Three commercial HDPE samples of granular shape were used in this study. The characteristics such as density and melt flow index (MI) measured under standard conditions ($P = 2.16$ kg, $T = 190^\circ\text{C}$) of all polymer samples are summarized in Table I.

The test apparatus was a Rheovis 2100, a constant shear rate type capillary rheometer made by the Ceast Co. (Italy). The reservoir diameter was 9.5 mm; a pressure transducer was installed at the top of the piston to measure the total pressure in extrusion. A set of circular dies was used for these tests. The diameter was 1 mm, the length-diameter ratios (L/D) were 10, 20, 30, and 40, and the entry angle of these dies was 180° .

Extrusion experiments were carried out in which the test temperatures varied from 160 to 200°C and shear rates varied from 50 to 1000 s^{-1} , to investigate the rheological behavior of the sample melt. In addition, the extrudate surface was observed.

RESULTS AND DISCUSSION

Entrance Pressure Losses

When a polymer melt enters a capillary from a reservoir, an entrance convergence flow and corresponding entry pressure losses are produced due to the contraction of the channel cross section. It is

Table I Characteristics of the Samples

Sample	Supplier	Density	MI
A	Dealim Chemical	0.955	18
B	Exxon Chemical	0.980	20
C	Exxon Chemical	0.965	8

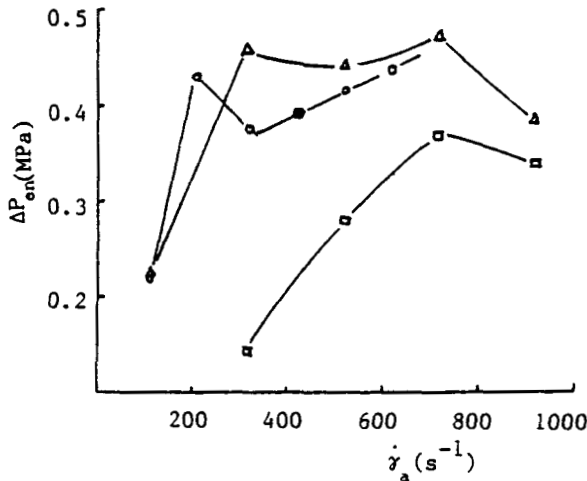


Figure 1 ΔP_{en} vs. $\dot{\gamma}_a$ for sample A: \circ , 160°C; Δ , 180°C; \square , 200°C.

generally considered that entry pressure losses are the sum of elastic stored energy and viscous dissipation in the polymer melt during extrusion. For a die with a large entry angle, the former effect is quite evident. The variance of entrance pressure drop, therefore, can be used to character the elastic behavior of polymer melt in entry flow. There have been a lot of empirical and semiempirical formulas to estimate or to predict the entry pressure drop for polymer fluids in extrusion and injection.⁹⁻¹² The Bagley plot method⁸ was used to determine the entrance pressure drop during extrusion of the samples in this paper.

Figures 1 and 2 show the dependence of entrance pressure drops (ΔP_{en}) on apparent shear rates

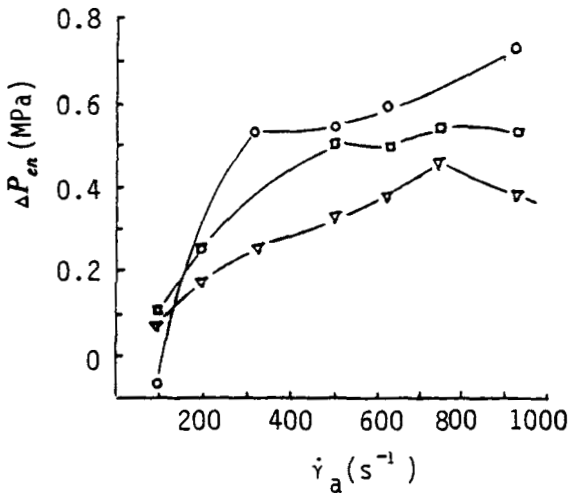


Figure 2 ΔP_{en} vs. $\dot{\gamma}_a$ for sample B: \circ , 170°C; \square , 190°C; ∇ , 200°C.

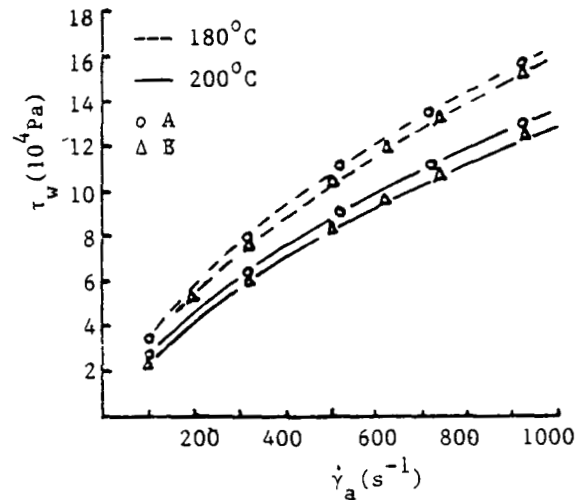


Figure 3 Apparent flow curves for the samples:

($\dot{\gamma}_a$) for samples A and B at the test temperatures, respectively. It can be seen that ΔP_{en} is very small during extrusion of the samples especially at low $\dot{\gamma}_a$ and high temperatures.

Sample Flow Properties

For the case of higher entrance pressure losses, the true shear stress at the wall can be expressed by the following formula:

$$\tau_w = (\Delta P - \Delta P_{en})R/2L \quad (11)$$

The apparent flow curves for the sample melts are shown in Figures 3 and 4 under the experimental conditions. It is found that the relationship between $\log(\tau_w)$ and $\log(\dot{\gamma}_a)$ is nearly linear, suggesting that

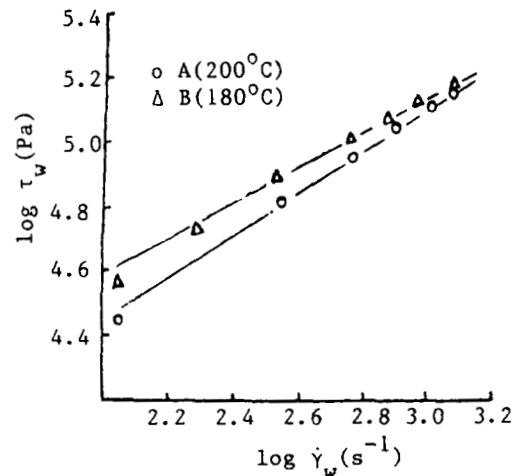


Figure 4 The sample flow curves.

the shear flow of the sample melts in the capillary extrusion does not strictly obey the power law.

Figure 5 shows the dependence of η_a on $\dot{\gamma}_a$ for the samples. It can be seen that η_a decreases with increasing MI at the same operation conditions and η_a is not much sensitive to $\dot{\gamma}_a$ for the material with lower MI such as sample C. Figure 6 displays the apparent shear viscosity curves of sample C at various temperatures. It is found that $\log \eta_a$ decreases with increasing $\log \dot{\gamma}_a$ when the temperature is constant; over a given range of shear rates, the relationship between $\log \eta_a$ and $\log \dot{\gamma}_a$ is also not linear. That is, the slope of the curves in various shear rate district is different; at lower shear rate ($\dot{\gamma}_a < 300 \text{ s}^{-1}$) the curves vary gently, and at higher shear rate ($\dot{\gamma}_a > 300 \text{ s}^{-1}$) the curves become steep. It suggests that the extrusion flow of sample C does not obey the power law.

The influence of temperatures on the apparent shear viscosity of the sample melts is shown in Figure 7. Under given shear rates, the apparent shear viscosity of the sample melts decreases with increasing temperatures, and the relationship between $\ln \eta_a$ and $1/T$ is basically linear. It means that the dependence of η_a of the sample on temperatures can be described by using the Arrhenius equation:

$$\eta = A \exp(E/R_0T) \quad (12)$$

where A is a constant which is related to material properties, E the activation energy for viscous flow, R_0 the universal gas constant, and T the absolute temperature.

It is found that the slope of the curve of $\ln \eta_a$ vs. $1/T$ of sample C is greater than that of samples A and B, suggesting that the value of E for sample C is higher than that of samples A and B. In other

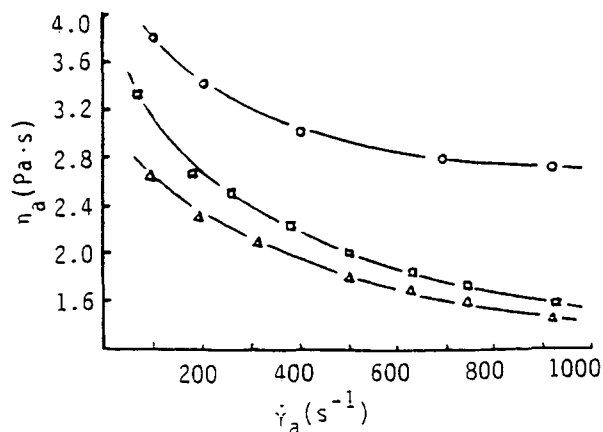


Figure 5 η_a vs. $\dot{\gamma}_a$ for the samples: \square , A; \triangle , B; \circ , C.

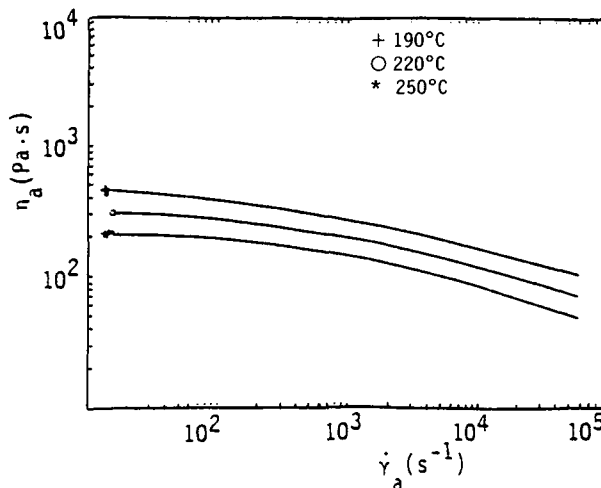


Figure 6 $\log \eta_a$ vs. $\log \dot{\gamma}_a$ of sample C. (Source: Exxon Chemical Company).

words, the apparent shear viscosity of sample C is more sensitive to temperature than that of the others.

Phenomenon of Shear-Induced Crystallization

It was found that when the entry pressure drops increased up to a certain value with increasing shear rate, it went down suddenly, and then increased gradually when the test temperatures were not high (lower than 190°C); as the temperature was higher (higher than 190°C), the curve of the entry pressure drop vs. shear rate had only one peak and the peak occurred at high shear rate (see Figs. 1 and 2). It seems that the sample melts take place during the shear-induced crystallization phenomenon. As

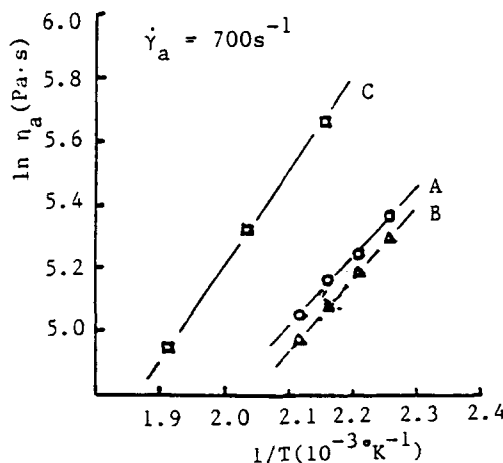


Figure 7 $\ln \eta_a$ vs. $1/T$ for the samples.

Table II The Critical Shear Rates ($\dot{\gamma}_{ac}$) of the Samples

Sample	Temperature (°C)	$\dot{\gamma}_{ac}$ (s ⁻¹)
A	160	219
	180	318
	200	721
B	170	318
	190	502
	200	743

mentioned above, the molecular chains of crystallizable polymer melt are stretched along the flow direction and produce orientation in entrance-converging flow. The part chains are folded as orderly structure to crystallize, and have flow resistance and pressure losses increased; thus shear stress also increases suddenly (see Figs. 3 and 4).

A study of morphology by Clark¹³ showed that the surface layer consists of row nuclei formed by chains aligned in the direction of flow; lamellae grew on them, and they were normal to both the surface and the direction of flow. From the viewpoint of macrorheology, the main factors affecting the phenomenon of flow-induced crystallization of crystallizable polymer are: temperature and temperature gradient; flow rate; channel geometry (includes entrance angles and contraction ratio of flow section). Under given conditions, the closer the operating temperature is to the melting point of material, the lower the critical flow rate of onset of flow-induced crystallization is; the higher the contraction ratio of flow section (or the larger the entrance angle), the more violent entry-converging flow and the higher the possibility of onset of flow-induced crystallization.¹⁴ Table II shows the critical shear rates of the onset of the flow-induced crystallization phenomenon of the sample melts under the experimental conditions. It can be seen that the critical shear rate decreases with increasing test temperature.

CONCLUSIONS

As to the macrorheology in polymer processing, the main factors affecting the flow behavior of HDPE melts are: temperature, shear rate (or shear stress), geometric parameters of the die (e.g., entry angle, diameter, and length), and pressure. It was found

that the sample melts showed shear-thinning behavior under the experimental conditions and the dependence of the sample melt viscosity on temperatures could be basically described by the Arrhenius equation. Strictly speaking, the melt flow of the samples in the die extrusion did not obey the power law; it was related to the flow-induced crystallization behavior of the sample melts during extrusion.

HDPE is a sort of linear crystallizability material. When a die with larger entry angle is used and the temperature approaches the melting point of the sample material to be processed, flow-induced crystallization can easily take place, even though the extrusion rate is low. It is worth considering this sort of materials as one selects processing parameters and performs processing procedure control.

REFERENCES

1. A. Keller and M. J. Machin, *J. Macromol. Sci. Phys.*, **B1**, 41 (1967).
2. R. R. Lagasse and B. Maxwell, *Polym. Eng. Sci.*, **16**, 189 (1976).
3. J. H. Southern and R. J. Porter, *J. Appl. Polym. Sci.*, **14**, 2305 (1970).
4. J. R. Collier, T. Y. T. Tam, J. Newcome, and N. Dinos, *Polym. Eng. Sci.*, **16**, 204 (1976).
5. G. Akay, in *Interrelations between Processing, Structure and Properties of Polymeric Materials*, J. C. Seferis and P. S. Theocaris, Eds., Elsevier, New York, 1985, pp. 669-686.
6. F. Morrison, G. Le Bourvellec, and H. H. Winter, *J. Appl. Polym. Sci.*, **33**, 1585 (1987).
7. J. L. White, in Ref. 5, pp. 145-156.
8. W. L. Wilkinson, *Non-Newtonian Fluids/Fluid Mechanics, Mixing and Heat Transfer*, Pergamon, London, 1960, p. 32.
9. E. B. Bagley, *J. Appl. Phys.*, **5**, 624 (1957).
10. F. N. Cogswell, *Polym. Eng. Sci.*, **12**, 64 (1972).
11. A. G. Gibson and G. A. Williamson, *Polym. Eng. Sci.*, **15**, 980 (1985).
12. J. Z. Liang, X. L. Sun, and G. J. Tang, in *Proceedings of China-Japan International Congress on Rheology*, Beijing University Press, Beijing, 1991, p. 190.
13. E. S. Clark, *Appl. Polym. Symp.*, **20**, 325 (1973).
14. Z. Tadmor and C. G. Gogos, *Principles of Polymer Processing*, Wiley, New York, 1979, pp. 65-70.

Received March 13, 1992

Accepted July 1, 1992